CHAPTER 2

CIRCULAR DATAIMAGE, A HIGH RESOLUTION CONTINUOUS IMAGE OF CIRCULAR-SPATIAL DATA

2.1 Introduction

The focus of this chapter is on a new method for imaging circular-spatial data, the circular dataimage. Figure 2-1 is a circular dataimage based on data introduced in Subsection 2.2.1 and further discussed in Section 2.4. The dataimage of Minnotte and West (1998), for the imaging of many ordered variables and observational units to show correlation structure, motivated the problem of how to image circular-spatial data and what this new method should be called. Moreover, dataimages for linear variables have been used extensively in various disciplines. Heatmaps, as they are called in genomics, have been made widely popular by Eisen, Spellman, Brown, and Botstein (1998).

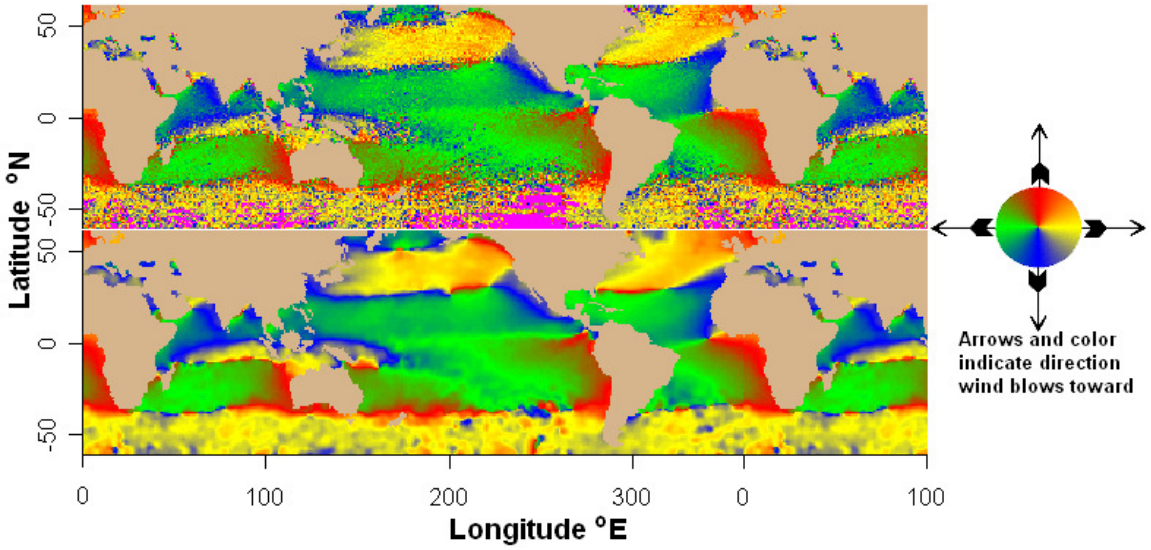

Figure 2-1. Circular Dataimages of the Direction Wind Is Blowing Toward, Coded with Yellow-Red-Green-Blue (YRGB) Color Wheel (Right). Average direction is shown in the top plot, and smoothed average direction in the bottom plot. The circular dataimage provides a continuous high resolution image of circular-spatial data with structure simultaneously recognizable on a broad range of scales.

This chapter is organized as follows: Section 2.2 introduces the data used throughout the chapter and provides an overview of some of the existing methods for the display of circular-spatial and vectorial-spatial data. Section 2.3 describes the “cross over” problem of circular data. Section 2.4 provides a solution to the cross over problem, the color wheel scale of direction, and the circular dataimage, with color continuity at the cross over point and capable of a high resolution image of circular-spatial data and statistics. Section 2.5 compares the circular dataimage with the existing method of arrow plots. Section 2.6 gives an example calculation of a circular color wheel for the Red-Green-Blue (RGB) color system. Section 2.7 provides color considerations, and color wheel and circular dataimage variations including a brief outlook of how magnitude might be encoded. Section 2.8 provides additional examples. Section 2.9 concludes with the summary and description of future work.

2.2 Overview of Vectorial-Spatial Displays

2.2.1 Data

The ocean wind data used throughout this paper were freely extracted from the International Comprehensive Ocean Atmosphere Data Set (ICOADS) at http://dss.ucar.edu/datasets/ds540.1/data/msga.form.html for the El Niño years 1972, 1976, 1982, 1987, 1991, 1994, and 1997, January through April, and in 1° increments for the area of longitude 0.5° E to +359.5° E by latitude -59.5° N to +60.5° N. Note that -3° N equals 3° south of the equator, and 359º E equals 1º W of the prime meridian. These data were selected to provide homogeneous data of the El Niño periods. El Niño (the child) refers to the Christmas season when changes in Pacific Ocean currents usually begin. These changes are often accompanied by severe climate disruptions to countries in and adjacent to the Pacific.

This dataset comprises 495,688 observations of month, year, longitude, latitude, and east and north components of wind velocity in units of 0.01 meters/second (m/s). With 0 to 28 observations per grid cell, average wind direction was computed as the quadrant specific inverse tangent of the average vertical component of wind velocity in a grid cell divided by the average horizontal component in the cell. Alternatively, hexagon binning has advantages for grouping data (Carr, Littlefield, Nicholson, and Littlefield 1987). All scaled figures in this paper have horizontal scale in º longitude and vertical scale in º latitude.

ICOADS began as COADS (Comprehensive Ocean Atmosphere Data Set) in 1981 as a cooperative project of the National Climatic Data Center (NCDC), the Environmental Research Laboratories, the Cooperative Institute for Research in Environmental Sciences, and the National Center for Atmospheric Research. COADS was renamed ICOADS in 2002 to recognize extensive international collaboration. The objective of ICOADS is to provide a consistent and easily used historical record of surface marine data beginning 1854. Seventy million unique reports of 28 variables obtained from ships of opportunity and ocean buoys were organized and cleaned of outliers. Trimmed monthly summaries give statistics for observed air and sea surface temperatures, wind east and north components in m/s, sea level pressure, humidity, cloudiness, and derived variables.

2.2.2 Smoothing Average Wind Data

The bottom subplot of Figure 2-1 and Figure 2-2 displays smoothed average wind data. The R package fields (Fields Development Team 2009) function image.smooth with a smoothing bandwidth of 2.5º was applied separately to the cosines and sines of average wind direction to avoid the cross over problem (see Section 2.3,

Crossover). The smoothed direction was computed as the inverse tangent of the smoothed vertical component divided by the smoothed horizontal component.

2.2.3 Existing Methods for Displaying Circular and Vectorial-Spatial Data

Some methods for the display for circular-spatial and vectorial-spatial data are shown in Figure 2-2. These methods were adapted from Ware (2004, pp. 200-205) using the R code in Appendix K.7. In all vectorial, arrow, and triangle icon plots in this and other chapters, flow or direction will be from tail to head. Figure 2-2 contains plots of:

a) Arrows of fixed length on a regular grid (Figure 2-2 (a)).

b) Jittered arrows of fixed length (Figure 2-2 (b)). Jittering is implemented here by adding values from a uniform distribution to the tail coordinates of the arrow. Thus, jittering only randomizes the origin of the arrow so jittered arrows have the same directions as nonjittered arrows. This helps to reduce overplotting and improves the sense of flow. Note that sufficiently large magnitude jitter can randomize the structure in directional-spatial data.

c) Jittered arrows of length proportional to magnitude (Figure 2-2 (c)).

d) Jittered triangle icons with icon area equal to vector magnitude (Figure 2-2 (d)).

Other methods discussed in Ware (2004, p. 204), but not shown, include: line integral convolution and large arrow heads along a streamline using a regular grid. Ware (2004, p. 205) stated "the display problem becomes ... to reveal important aspects of the data for a particular set of tasks ...." So, the choice and effectiveness of a method depends on the task to which the method is put. Within this paper, the task is to discover structure in circular-spatial data (all vectors have equal length). Hence, the circular dataimage will be compared to plots of arrows of equal length (method a).

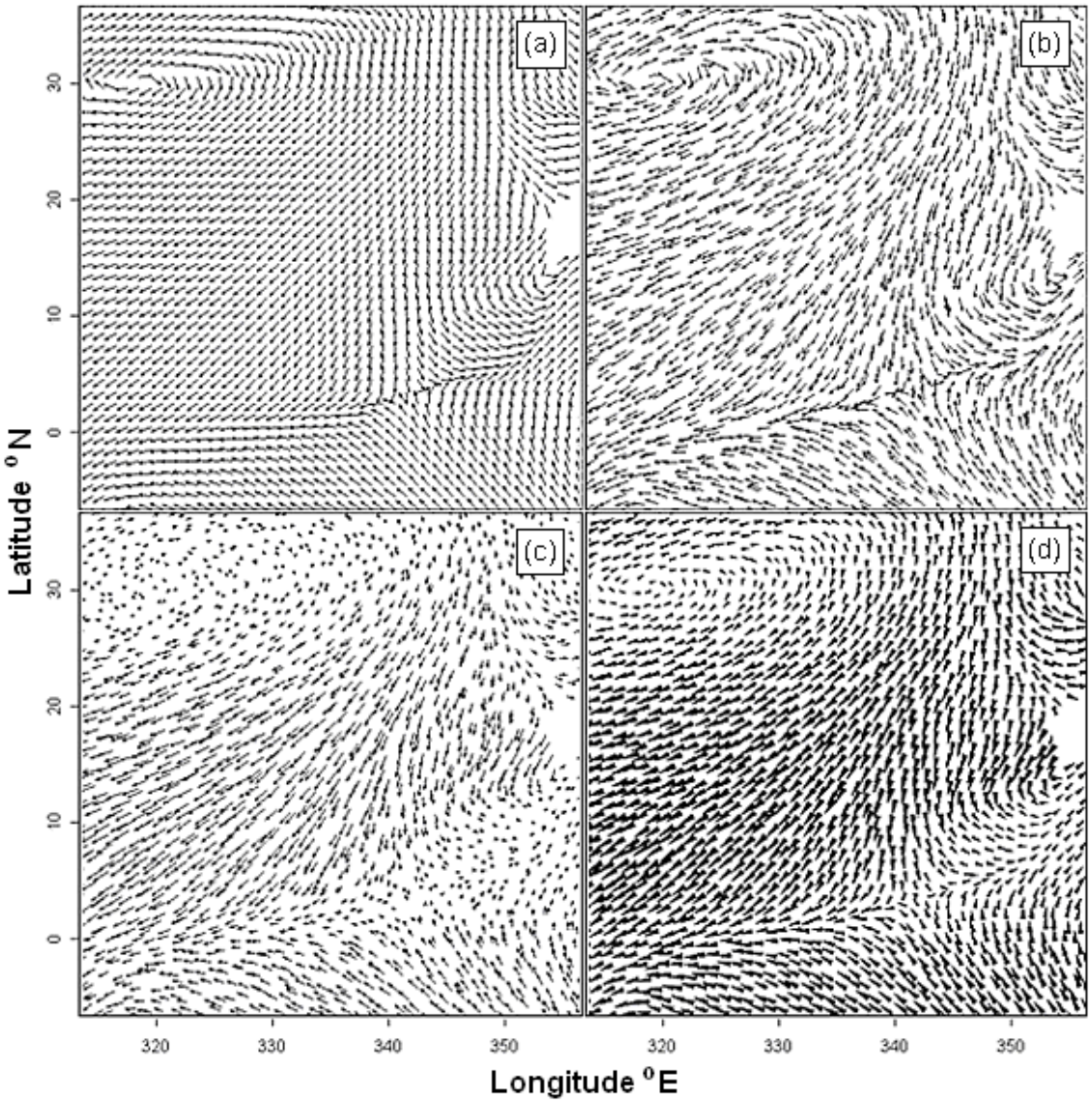

Figure 2-2. Some Existing Methods for Display of Circular and Vectorial-Spatial Data Using the Smoothed Ocean Wind Data. (a) Unit vectors, (b) jittered unit vectors, (c) jittered vectors, (d) jittered triangle icons with icon area equal to vector magnitude. Jittering helps to reduce overplotting improving the sense of flow.

2.3 Cross Over

Circular data, as opposed to linear data, is cyclic, i.e., the starting point at 0º equals the ending point at 360º. The distance between values of 0 and 360 on a linear scale is 360, but the distance on a circle between 0º and 360º is 0°. The distance on a unit circle between 0 and 2π radians is 0 radians. In 1802, John Playfair noted that directional data should be analyzed differently from linear data, recommending that the average direction should be the direction of the vector resultant. Thus, the average or central direction of 1° and 359° is not the arithmetic mean of 180°. The correct average is 0°, which is equal to the direction of the sum of the unit vectors (cos 1°, sin 1°) and (cos 359°, sin 359°). Summing these unit vectors, the equal and opposite vertical components annihilate and the equal horizontal components reinforce.

Historically, this problem arose in automating the summarization of wind data. It has been called the “cross over” problem because it occurs when crossing over 360° on a scale of 0° to 360°, or crossing over +180° on a scale of -180° to +180°. In another example, cross over occurs in plotting a circular time series with direction on the vertical axis and time on the horizontal axis. As direction rotates counterclockwise (CCW) past 360º, direction vanishes at the top of the scale at 360° and instantly reappears at the bottom of the scale at 0° at the next time value resulting in a full scale vertical gap between plotted points. In vector field visualization, when direction is coded with a single color gradient, e.g. dark blue at -180° to bright red at +180°, image discontinuity occurs where direction varies around 180°. At the cross over point the direction to color correspondence is one to two. An image using this scale would display the 180º direction as either red or blue depending on whether direction is increasing or decreasing. To avoid this problem, users may examine subregions where cross over

does not occur. Consequently, the ability to resolve both local and global structure in circular-spatial data is reduced, and the overall structure is not seen.

2.4 The Circular Dataimage and Color Wheel

2.4.1 The Color Wheel Solution to Cross Over

Suppose that a linear color scale, made from a blue-red color gradient to code direction from -180º to +180º (Figure 2-3 (a)), is wrapped on a circle with -180º (blue) connected to +180º (red) on the left side of the circle. A red-to-blue color discontinuity occurs at the cross over point where the ends of the wrapped scale intersect at +/-180º (Figure 2-3 (b)). To eliminate the discontinuity, a three-color gradient, red to green to blue with continuity between gradients, was inserted and centered at +180º. In Figure 2-3 (c), each two-color gradient (green-blue, blue-red, red-green) is adjusted to an equal arc length of 120º. Every point on the color wheels (c) and (d) is color continuous. The color scheme in (b) is discontinuous at the 180º location.

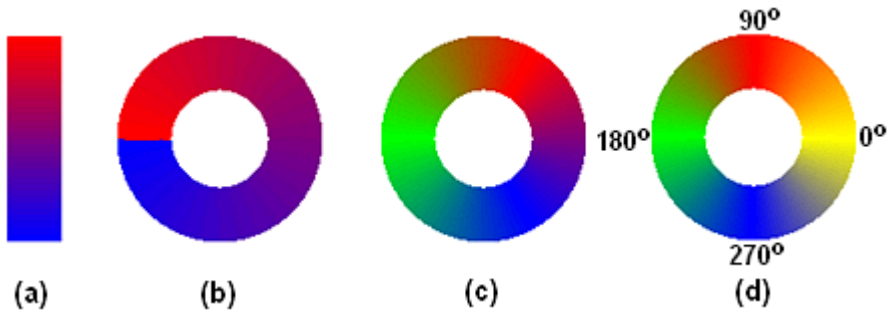

Figure 2-3. Evolution of the YRGB Color Wheel. (a) Blue-red linear color scale, (b) color scale (a) wrapped on circle, (c) red-green-blue linear color gradient inserted at 180º, and (d) blue-yellow-red gradient inserted at 0º and labels added. The final YRGB color wheel (d) aligns the 4 main colors (yellow, red, green, and blue) to the 4 main directions (0º, 90º, 180º, 270º).

An additional blue-yellow-red color gradient was inserted at 0º and the component two-color gradients (green-blue, blue-yellow, yellow-red, red-green) were adjusted to 90º arcs (Figure 2-3 (d)). This particular color wheel is called a YRGB Color Wheel. The four-color color wheel is more intuitive than the three-color color wheel because the number of main or pure colors between color gradients equals the number of main directions (0º, 90º, 180º, and 270º, or east, north, west, and south), aligning the four main colors to the four main directions. Thus, the information (number of perceived color boundaries and degree of color structure) in the dataimage (Subsection 2.4.2) of circular-spatial data is increased. In general, a color wheel can be defined as a sequence of three or more two-color gradients with color continuity between connecting color gradients. Hence, the color wheel is color continuous at any point on the color scale going clockwise or counterclockwise.

2.4.2 The Circular Dataimage

To image circular-spatial data, let a direction in a pixel be plotted as the color on a color wheel in the direction of the data. The result is called the circular dataimage. In all circular dataimages in this and other chapters, flow or direction will be from the center of the color wheel toward the color on the color wheel. In Figure 2-1, which was constructed using the R code in Appendix K.2, the average direction that ocean wind blows toward is coded with the YRGB color wheel at the right. The YRGB color wheel consists of color gradients yellow to red from 0° to 90°, red to green from 90° to 180°, green to blue from 180° to 270°, and blue to yellow from 270° to 360°. The resulting circular dataimage shows some interesting features. In the Pacific Ocean and around the equator, wind tends to blow from east to west, which is typical for any year. The pattern of direction on the west side of the Americas is similar to that on the west side of

Africa: wind flows toward the equator from both the north and the south, then turns to the west.

2.5 Comparison of Methods

Figures 2-4-1 and 2-4-2 show the direction ocean wind is blowing toward between 100º and 325º E longitude and between -59.5º and 60.5º N latitude. Figure 2-4-1 shows average direction as described in Subsection 2.2.1 computed with 0 to 28 observations of direction per location due to missing data. Figure 2-4-2 shows smoothed average direction as described in Subsection 2.2.2.

As black arrows were hardly visible in some regions when plotted on a dataimage using the previously discussed YRGB color wheel, direction is coded via the hue, saturation, and value (HSV) color wheel (saturation = 0.5) in the right margin of the subplots. Further discussion on various color spaces will be found in Subsection 2.7.1. Missing ocean data is coded by white, and structurally missing values over land by tan. Arrows are overplotted at a density of one arrow per 15 cells in the horizontal and vertical directions in subplots B and F, and at a density of one arrow per 5 cells in Subplots C, D, G, and H.

The ability to perceive structure via arrow plots depends on the variability of the data and the arrow density relative to the plot scale. In the relatively noisy latitudes south of Australia (135º E, -25º N) in Figure 2-4-1 B, the general direction of the arrows is difficult to recognize. The arrows point in random directions due to noise. Increasing the arrow density in Figure 2-4-1 C does not help. The arrows are more misleading than informative. The use of arrows alone on noisy data in Figure 2-4-1 D is worse.

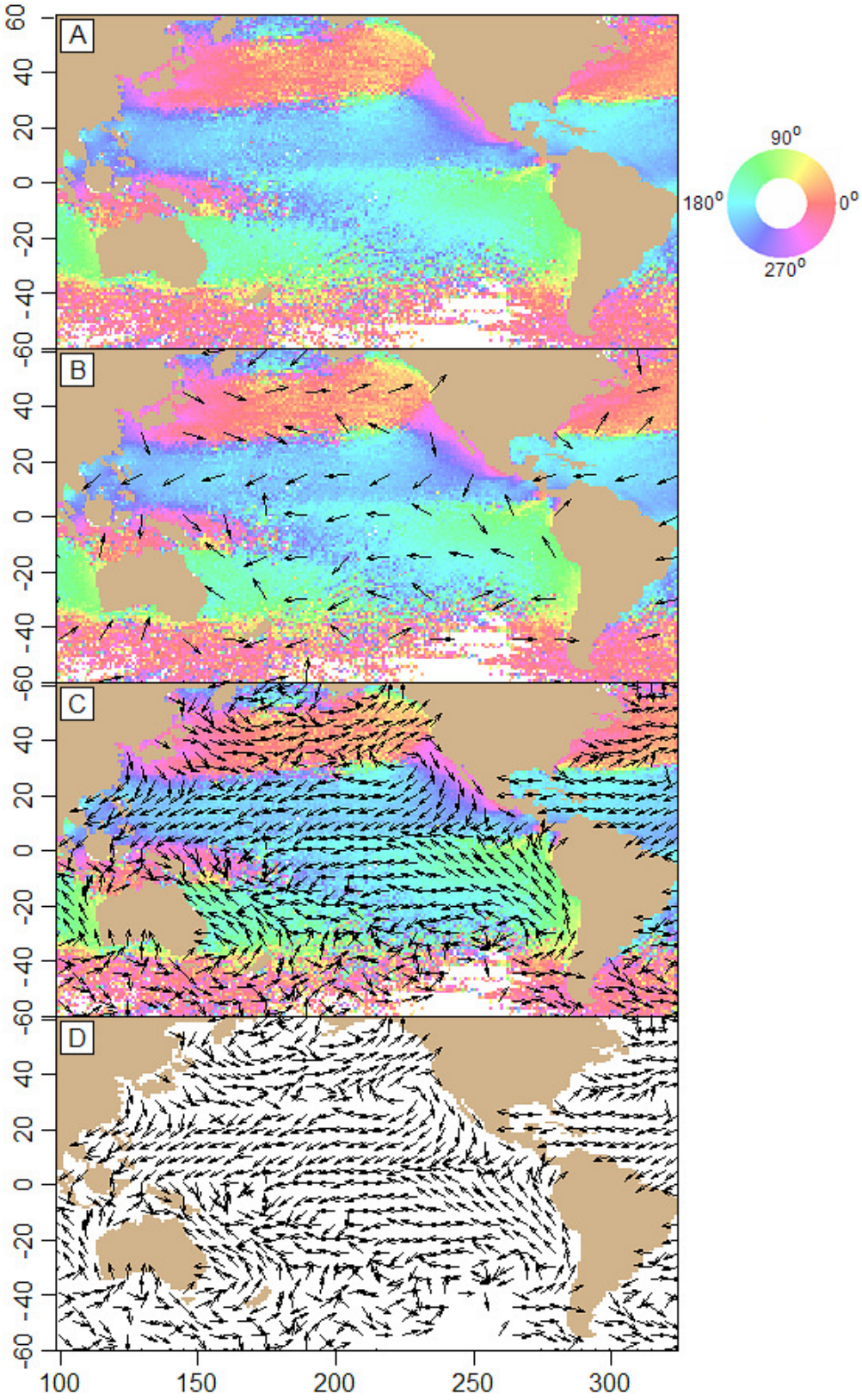

Figure 2-4-1. Plots of Average Ocean Wind Direction.

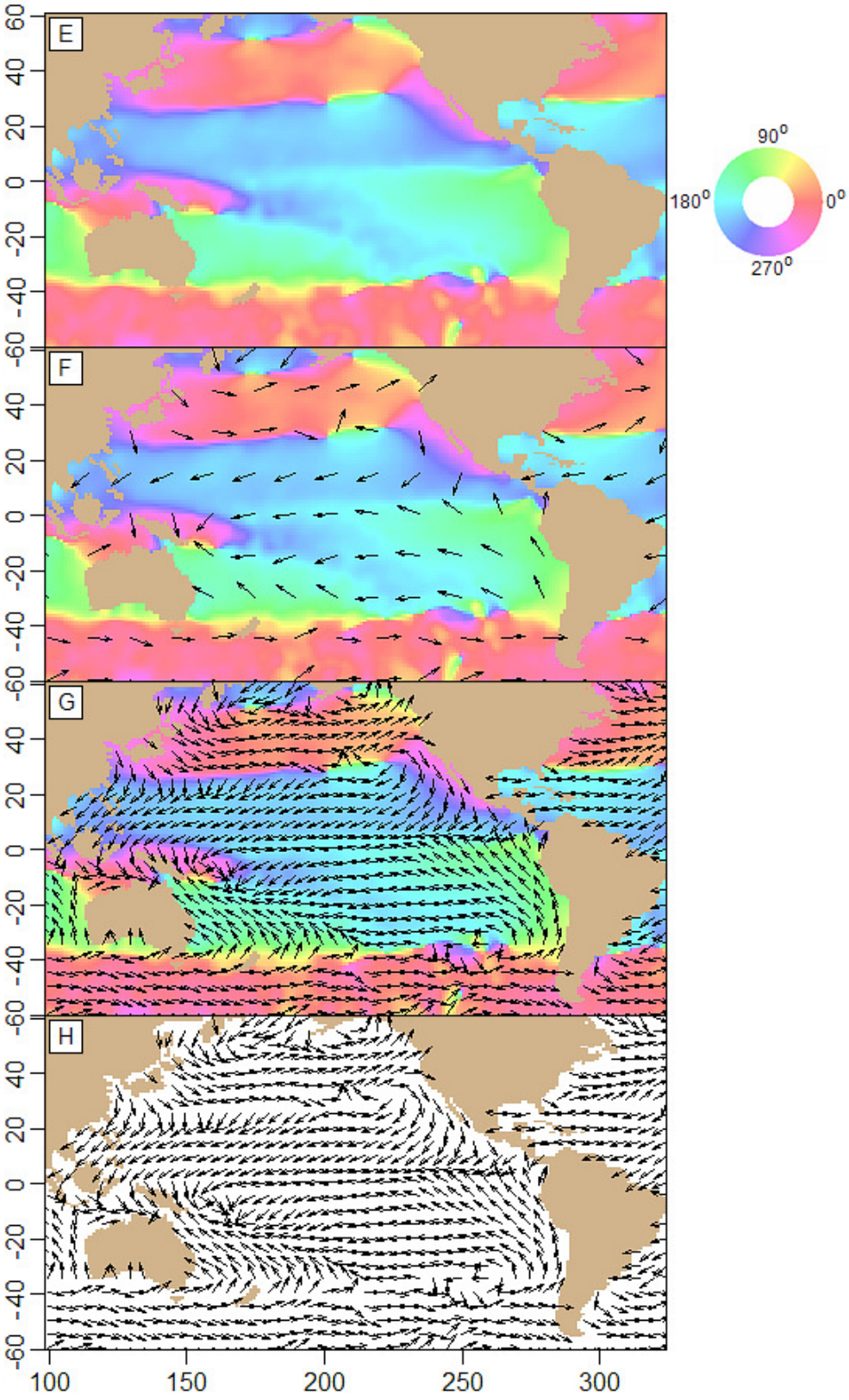

Figure 2-4-2. Plots of Smoothed Ocean Wind Direction.

In Figure 2-4-2 the data are smoothed, which replaces missing values. Figure 2-4-2 E shows maximum structural detail. In Figure 2-4-2 F the general direction in the extreme southern latitudes is apparent in the arrow structure. Increasing the arrow density on the smoothed data in Figure 2-4-2 G or using arrows alone in Figure 2-4-2 H further increases the perception of structure. Arrows work well for smooth data at low to moderate arrow density.

In contrast, the circular dataimage shows more structure in noisy data. The general direction in the latitudes south of Australia can be seen as the dominant color in Figure 2-4-1 A as approximately west to east. The colors alone in Figure 2-4-1 A give a better overall impression of the structure, general direction, noise, and missing data than colors and arrows in Figure 2-4-1 B.

Figure 2-5 shows average wind direction coded with the Blue-Green-Yellow-Red (BGYR) color wheel with missing values displayed in magenta (southern latitudes) and continents shown in tan. The data plotted in the left plots are identical to the data plotted in the right plots with decreasing scale (zooming in) top to bottom.

As we zoom into a smaller area, directional structure in the arrow plots eventually becomes recognizable, e.g., Figure 2-5 (e). With increasing scale (zooming out) and constant arrow spacing relative to the data, arrow plots eventually become unintelligible, e.g., in Figures 2-5 (a) and (c). In contrast, the circular dataimage shows overall and detailed structure on a wide range of scales, e.g., Figures 2-5 (b), (d), and (f). Even at a scale of a 50º x 50º area (Figure 2-5 (f)), the circular dataimage easily shows structure that is not easily obtained from the arrow plot in Figure 2-5 (e).

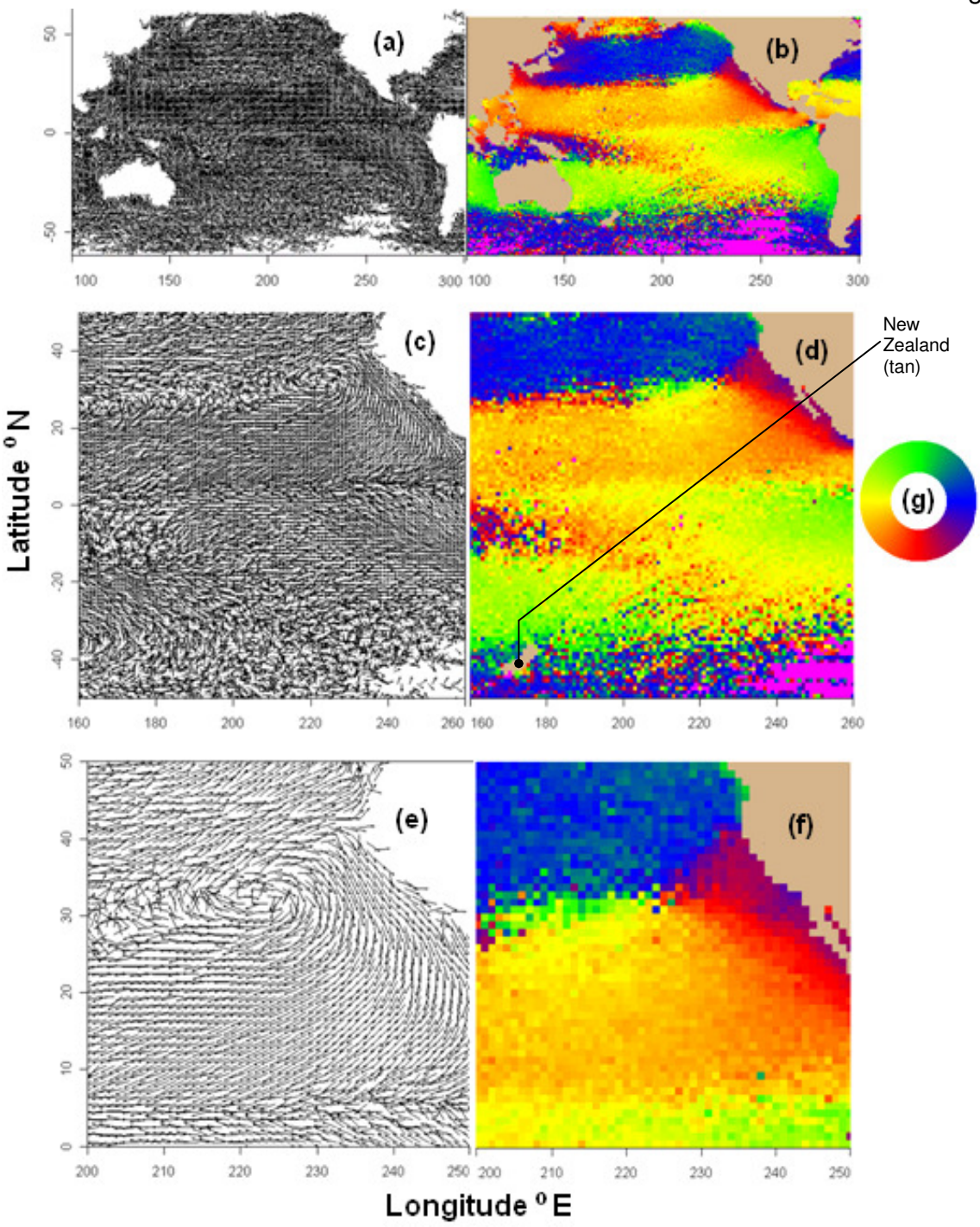

Figure 2-5. Comparison of Arrow and Circular Dataimage Plots of Average Ocean Wind Direction. Plots (a) and (b) cover 200º of longitude; (c) and (d) cover 100º Of longitude; (e) and (f) cover 50º of longitude; and (g) BGYR color wheel. The ability to recognize structure depends on plot type, smoothness of data and density and arrows, and distribution of missing data.

Additional characteristics of circular dataimages and arrow plots include:

- Missing values can easily be seen as a contrasting color not in the color wheel, or by plotting arrows over missing data plotted as an area in contrasting color.
- Arrows may overplot and obscure geographical boundaries as in Figure 2-5 (c) (New Zealand obscured), but boundaries may be overplotted on circular dataimages. New Zealand remains visible in (d).
- Circular dataimages fill the plot at pixel level resolution. Arrows cannot.

The circular dataimage has been defined, compared with arrow plots, and its capabilities have been demonstrated. In Sections 2.6 and 2.7, the use of color will be discussed in further detail.

2.6 Calculation of a BGYR Color Wheel

Table 2-1 shows how the color levels of red, green, and blue on a scale of 0 to 1 were computed for the BGYR color wheel in Figure 2-5. For example, as direction goes CCW from 0° to 90°, the corresponding color is obtained by decreasing the amount of blue and increasing the amount of green linearly while the level of red is constant at zero. The reader is invited to experiment with nonlinear color gradients.

Table 2-1. BGYR Color Wheel Formulae for RGB Space.

Angle (°) in	Color Range	Level of Red	Level of Green	Level of Blue
[0,90)	blue to green	0	Angle / 90	1 – Angle / 90
[90,180)	green to yellow	(Angle - 90) / 90	1	0
[180, 270)	yellow to red	1	1 - (Angle - 180) / 90	0
[270, 360)	red to blue	1 - (Angle - 270) / 90	0	(Angle - 270) / 90

2.7 Color Considerations and Variations

2.7.1 Color Space

The use of color in computer graphics is described in Foley, Van Dam, Feiner, and Huges (1992). The use of color in presentation graphics is described in Ihaka (2003). The use of color in statistical graphics is described in Zeileis, Hornik, and Murrell (2008). Color spaces include CIEXYZ, RGB, HSV, CIELUV, and HCL. CIEXYZ is one of the first color spaces based on measurements of visual perception and mathematically defined. CIE denotes the Commission Internationale de l'Éclairage, 2004, which is an international body of scientists whose standards provide for the accurate communication of color information. X, Y and Z values are the levels of the primary colors added to match a color. RGB is a version of CIEXYZ space. R, G, and B are the relative intensities of the red, green, and blue primaries. HSV is a transformation of RGB space to hue (H), saturation (S), and value (V). However, HSV colors are often not considered to be perceptually based because the brightness of colors is not uniform over hues and saturations. CIELUV is a transformation of the CIEXYZ space to the perceptual axes of luminance, and the coordinates *u* and *v* of the CIE chromaticity map of human color perception. HCL colors are obtained by transforming the rectangular coordinates of *u* and *v* in the CIELUV space to the polar coordinates of hue H and chroma C. Hue H takes values in the range 0 to 360º with 0º = red, 120º = green, 240º = blue, etc. Within the space's boundaries, the admissible levels of chroma and luminance depend on the hue chosen as some hues lead to light and others to dark colors.

The R contributor package colorspace (Ihaka, Murrell, Hornik, and Zeileis 2009) includes the above color spaces together with a variety of HCL based qualitative palettes for categorical data, and divergent and sequential palettes for numerical data. The colors of a color wheel, when applied to directional data, define a new class of palette,

the circular palette. The color wheels in this paper use color in the RGB and HSV color spaces. Color wheels based on the HCL color space were not included because they are less effective in highlighting and contrasting circular-spatial structure. Kosara, Healey, Interrante, Laidlaw, and Ware (2003) recommend a color sequence with a substantial luminance component to reveal form or if detailed patterns need to be displayed.

2.7.2 Color Functions

Different color gradients, different color gradient orders, nonlinear gradients, and/or color spaces may be more effective in a particular application. For scientific visualization, Brewer (1997, p. 210) suggested the spectral sequence of red purple, red, orange, yellow, green, blue, and purple to arrange adjacent darkest and lightest colors which mark hue changes to form visually prominent color boundaries through the color sequence. The modified spectral sequence of purple, red, orange, yellow, green, and blue divides the angular range into convenient 60° bins or gradients while enjoying most of the benefits of the Brewer spectral sequence. A diverging color sequence focuses attention on a band of directions. Other color schemes recommended by Brewer (1997) can be obtained from the ColorBrewer software tool at http://ColorBrewer.org.

Another function of color is to distinguish among nonstructural missing data (missing ocean data), structurally missing data (land areas), and nonmissing data. In the figures of this paper, structurally missing data over the landmasses, which results in the well known shape of the continents, are indicated by tan, and missing ocean data (most notably in the regions around the South Pole) are indicated by grey or magenta colors. If possible, colors for missing data should not duplicate colors for nonmissing data. Generally, for structurally missing data over a large area, we suggest neutral colors, e.g.,

tan (sandy brown), which do not duplicate color wheel colors for data and are comfortable to view compared to an intense color like dark blue.

Various forms of human color impairment exist. Deuteranopia (reduced capability to see green) affects about 5% of males and about 0.5% of females. Protanopia (reduced capability to see red) affects about 1% of males. The tritanopic has reduced capability to see blue. Colors for the color impaired are described at http://www.toledo-bend.com/colorblind/index.asp. For people with red or green color deficiency, Brewer (1997) recommended the spectral sequence red, orange, yellow, blue-green, blue, and purple-blue (ROYBgBPb).

In Figure 2-6, the bottom plots are based on a ROYBgBPb color scale (purple-blue was coded as red + blue). The top plots are based on the Green-Yellow-Red-Blue (GYRB) color scale. To view these images as a color-deficient person would see them, jpeg graphics were uploaded to http://www.vischeck.com/vischeck/vischeckImage.php. To the deuteranopic, the left side of Figure 2-6 appears as on the right side. The bottom right plot, with yellow-grey-light blue-blue, shows more structure than the upper right plot with indistinguishable yellows for red and green. Using the Vischeck simulation, colors may be varied to develop better color scales for the color impaired.

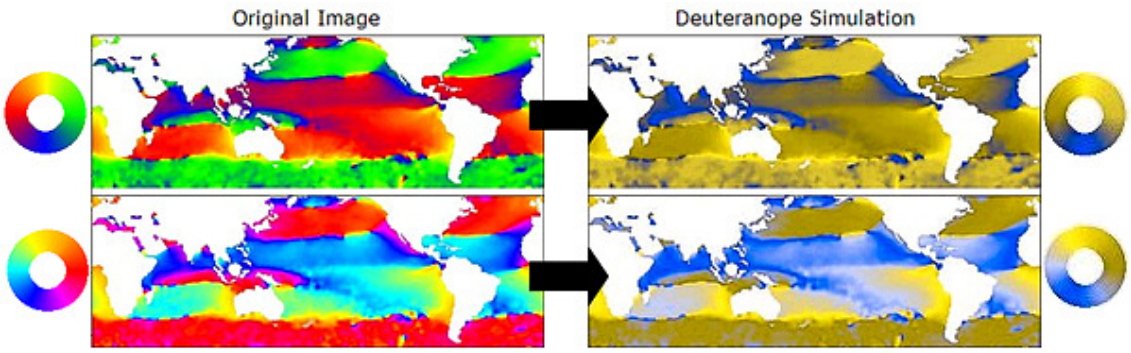

Figure 2-6. Normal and Simulated Deuteranopic Views of Images. To the deuteranope, the left plots appear as on the right with red and green being indistinguishable.

2.7.3 Color Wheel Variations

Figure 2-7 displays a variety of suitable color wheels in the RGB color space to show some of the many possibilities and to motivate experimentation to discover interesting structure in circular-spatial data. The top labels indicate which colors are used. From left to right, the continuous color wheels include the GYRB, the Black-Blue-White-Red (KBWR), and a modified Brewer Divergent, and the discrete color wheels include a modified Brewer Divergent, the KBWR, and the Rainbow color wheel. The modified Brewer divergent color wheels were constructed by connecting the ends of the Brewer 10-color divergent sequence #6 at http://ColorBrewer.org together, and replacing the dark color at one of the ends with an average of the dark colors at both ends. The KBWR discrete sequence was constructed from main colors of black, blue, white, and red inserting intermediate colors 1/3 and 2/3 of the way between main colors by varying levels of red, green, and blue. Brewer's (1994) 3 x 3 arrays of color in "generalized set of color schemes" at http://www.personal.psu.edu/cab38/ColorSch/Schemes.html provide additional sequences for discrete color wheels by omitting the center color, or by cycling around a pair of adjacent rows or columns.

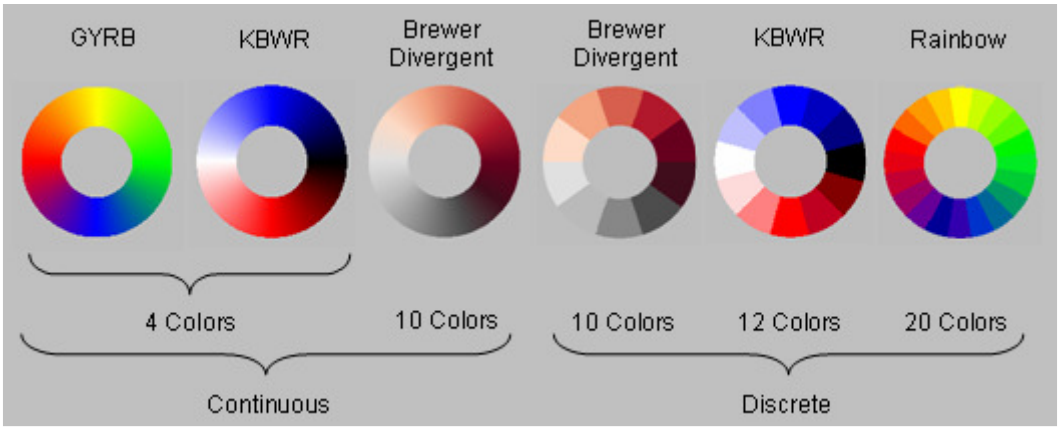

Figure 2-7. Variety of Continuous and Discrete Color Wheels.

Figure 2-8 shows the effects of different continuous and discrete color wheels on noisy and smoothed data. The continuous color wheels produce smoother overall pictures with "soft" or fuzzy color boundaries and show maximum directional detail. The discrete color wheels provide for exact quantification of regions with similar values via "hard" color boundaries between adjacent ranges of direction. Color wheels with 20 bins show more directional detail than color wheels with 10 or 12 bins. Similar to histogram binning, the appearance of the image will vary with the choice of the bin origin and the bin width. The choice of discrete or continuous color wheel depends on the function of the circular dataimage.

More color wheels and effects can be obtained by rotating a color wheel. In Figure 2-9, the amount and direction of rotation is shown at the center of the GYRB color wheels. Missing values are indicated by magenta and tan, which are not in the color wheel. For focus on the equatorial region using the GYRB color wheel, the bottom plot (90º) is best and top plot worst. In the bottom subplot, yellow at 180º indicates wind blowing from east to west. The adjacent colors of green or red shade yellow to indicate deviations toward the north or south, respectively. Choose a rotation that best contrasts and highlights structure in an area of interest and is comfortable to view.

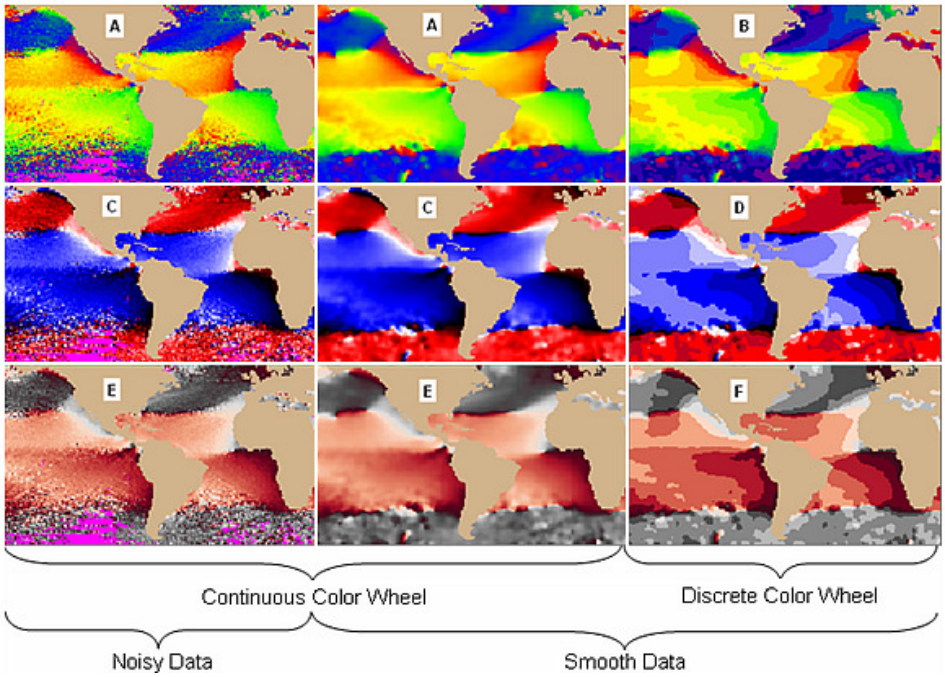

Figure 2-8. Effects of Color Wheel and Smoothness of Data. Color scales rotated 90º: (a) GYRB; (b) rainbow; (c), (d) KBWR; (e), (f) Brewer divergent. Choice of a color wheel depends on the objective of the circular dataimage.

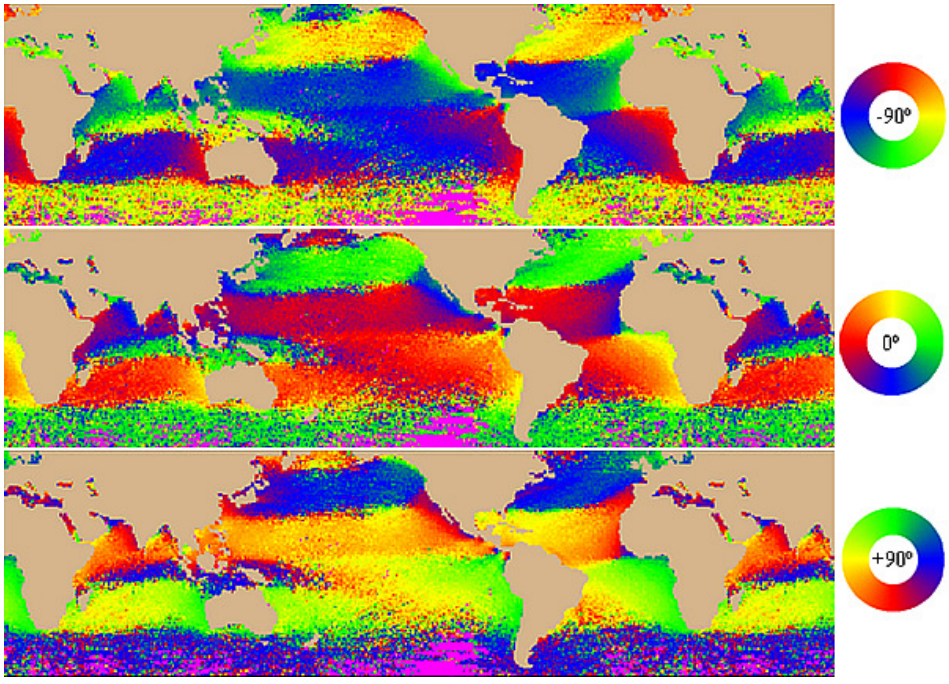

Figure 2-9. Effects of Color Wheel Rotation, Color Wheel Labeled with Rotation. The color wheel is rotated to effectively highlight structure in an area of interest. For focus on the equator using the GYRB color wheel, the bottom plot is best and top plot worst.

2.7.4 Summary of Benefits to Be Obtained from Using Different Color Schemes

- The Brewer spectral scheme red-purple, red, orange, yellow, green, blue, and purple forms visually prominent color boundaries adding structure to the circular dataimage.
- Diverging color schemes focus attention on a band of directions (Figure 2-7, middle four color wheels, and Figure 2-8, bottom).
- Colors not contained in the color wheel can be used to distinguish nonstructural missing data (e.g., missing ocean data), and structurally missing data (e.g., land areas) from nonmissing data (Figure 2-8). Neutral colors that are not used in the color wheel, e.g., tan, do not distract from colors used for data. A contrasting color not in the color wheel makes it easy to see missing data.
- The continuous color wheels give "soft" color boundaries and show maximum detail (Figure 2-8, left and middle plots). The discrete color wheels give “hard” color boundaries for the exact identification and quantification of regions with similar values (Figure 2-8, right plot) for low to moderate number of colors.
- Rotation helps to select a color sequence that contrasts and highlights structure in an area of interest (Figure 2-9, bottom, for the equatorial region). Changing from a light color, e.g., yellow or green, toward a dark color, e.g., blue or red, seems to be more effective than changing from a dark color toward a light color. Special color sequences and rotations increase the ability of color impaired viewers to recognize structure in an area of interest.

2.7.5 Circular Dataimage Variations

A single gradient of color could be used to interactively focus on a range of directions. Using the single color gradient black to white with black for the main direction and vanishing to white at 45º (or another arbitrarily selected cutoff) away from the main direction will give some sense of where the main direction lies, show some structure related to the main direction, and eliminate structure in the vanished areas.

Figure 2-10, which is here named a "focus" plot, augments the black-white color gradient by highlighting in green any direction that is within a tolerance of the main direction. Interactively, the user enters a "focal" direction and a tolerance in degrees (º). In the bottom plot of Figure 2-10, the focal direction is 180º for wind blowing from the east to the west and the tolerance is 1º. The green pixels represent areas with directions in the range of 179º to 181º. The white areas have directions more than 45º away from the focal direction.

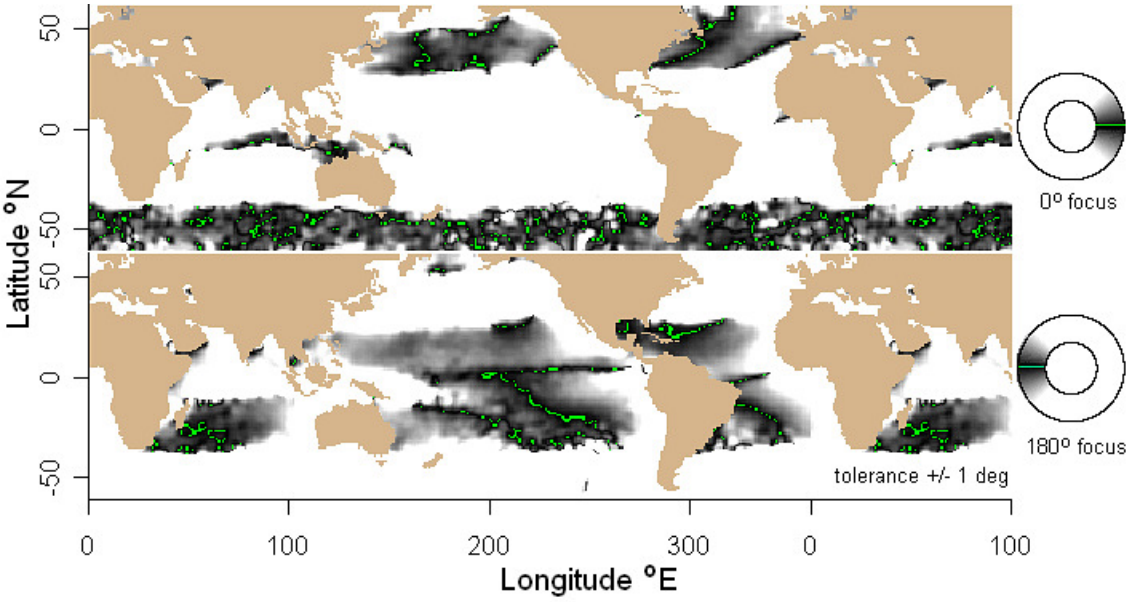

Figure 2-10. Focus Plots of Smoothed Average Direction with Focal Directions 0 º (Top) and 180 º (Bottom). Shading fades to white at 45º from focal direction. Areas within 1º tolerance of focal direction are colored green.

An axial random variable takes a random axis orientation when there is no reason to distinguish a direction from its opposite direction, e.g., fault lines. Figure 2-11 illustrates an axial focus plot of wind direction that highlights two specific axial directions or orientations. The top of Figure 2-11 combines the top and bottom of Figure 2-10 in one single plot. While this plot type is not particularly useful for the running example of ocean wind data, such a plot will make much more sense for true axial-spatial data.

Overall, this chapter has dealt with direction. Magnitude will now be briefly discussed. The use of arrows to represent direction and strength has been common practice. For example, see the "Vector Maps" at http://www.ssg-surfer.com/html/surfer_details.html (Scientific Software Group 2008). In CFD visualization, 3D perspectives of the paths of particles in a flow are colorized by magnitude, e.g., temperature or pressure. For example, see the flow curves at http://www.fluent.com/solutions/examples/x209.htm.

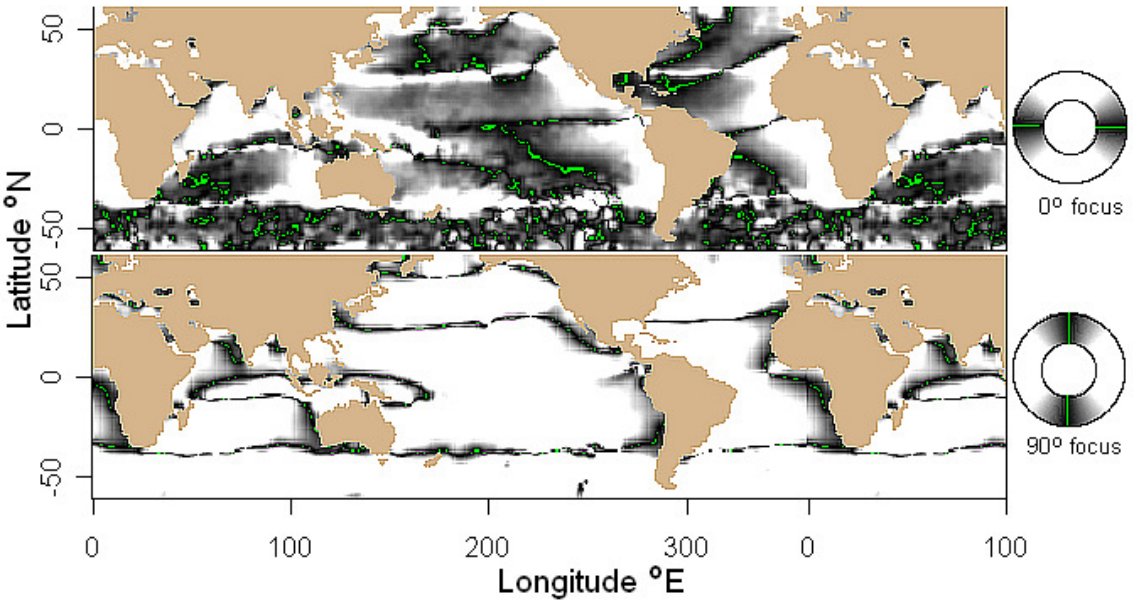

Figure 2-11. Axial Focus Plots of Smoothed Average Direction with Axial Focal Directions 0 º (Top) and 90 º (Bottom). Shading fades to white at 45º from focal direction. Areas within 1º tolerance of focal direction are coded green.

Going from arrows to the circular dataimage, vector magnitude is lost. However, circular dataimages can be enhanced with magnitude information. Suggestions include representing magnitude using alpha-blending or lightness. In Figure 2-12, wind speed is binned by quartiles and coded as quarter values (V) of the HSV scheme. Direction is binned in 45º intervals and coded as hue (H) in 45º increments. The outer ring represents the fourth quartile of wind strength. This enhancement provides some useful strength structure. Visual extraction of direction and strength was difficult when binning strength by few levels of value with hue a continuous function of direction. Hence, a few levels of value and a few levels of hue are suggested. Traditional methods, e.g., adding contour curves such as in Figure 2-13, adding arrows of variable length corresponding to magnitude to a circular dataimage, or adding a heatmap (linear dataimage) of magnitude to the side of a circular dataimage are effective.

Finally how can the circular dataimage be used to discover new patterns? Changes in pattern may be discovered by imaging the difference of directions with respect to two conditions, e.g., El Niño periods vs. other periods, and looking for changes in shape and color.

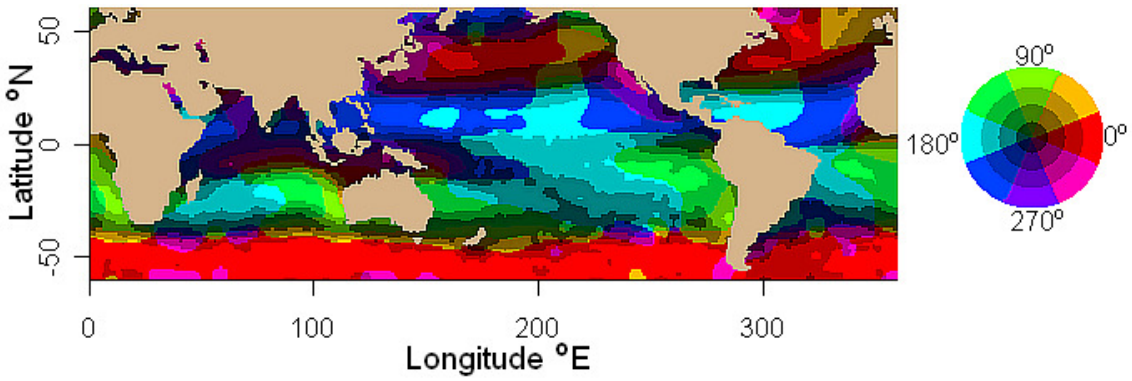

Figure 2-12. Strength Binned by Quartiles and Coded as Value (V) in HSV Scheme. In the color wheel, value increases from center outward in quarters corresponding to strength in quartiles. Direction is binned by hue into 45º bins.

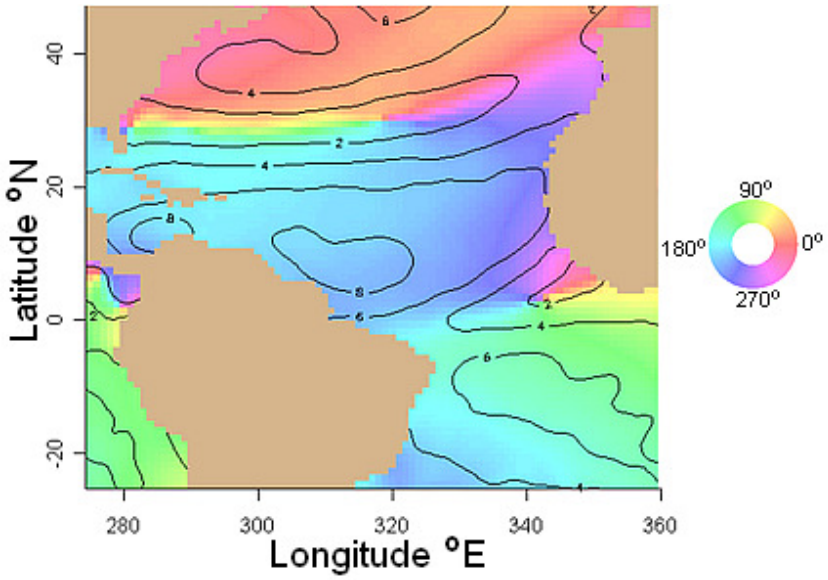

Figure 2-13. Circular Dataimage of Wind with Direction Coded Using HSV Color Wheel and Magnitude (m/s) Plotted as Contour Curves.

2.8 Other Examples

2.8.1 Earth Main Magnetic H Field Direction

The International Geomagnetic Reference Field (IGRF) models in Figures 2-14 and 2-15 were extracted without cost from the National Geophysical Data Center (NGDC) at http://www.ngdc.noaa.gov/geomagmodels/IGRFGrid.jsp. The scientific domain of the NGDC spans the distance from the bottom of the sea to the surface of the sun, providing data describing the marine, solid Earth, and terrestrial-solar environments. The total magnetic field at any point on the Earth's surface derives from multiple sources. The main field, which generates more than 90% of the total field, is generated in Earth's outer core. For more information, go to Frequently Asked Questions at http://www.ngdc.noaa.gov/geomag/faqgeom.shtml.

Figures 2-14 (a) to (c) image the direction of the Earth main magnetic horizontal (H) field for 9/15/2004 and elevation 0 km using 65,340 observations of longitude, latitude, and east and north components of the magnetic field in nano Tesla (nT).

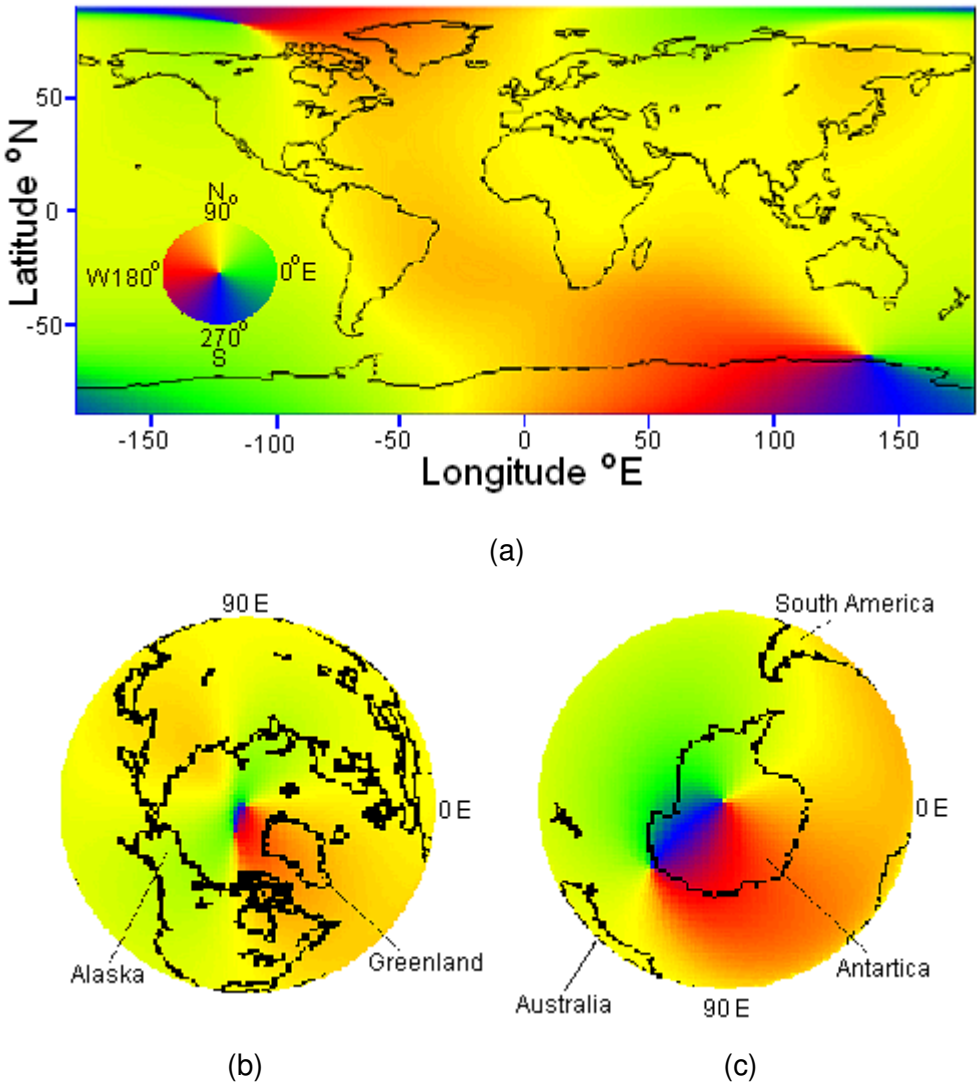

Figure 2-14. Circular Dataimage of Earth Main Magnetic H Field Direction. IGRF model for elevation 0 km on 9/15/2004 with a GYRB color wheel (green = East = 0°).

The choice of GYRB color wheel results in subtle green and red color shadings around yellow to emphasize north and show directional detail. In Figure 2-14 (a), the backward "S" shaped yellow band crossing North and South America codes north. The rectangular plot distorts the pattern of direction, especially at the poles. Figures 2-14 (b) and (c) correct this distortion by mapping the color onto a sphere and displaying it in perspective (spherical circular dataimage). Figure 2-14 (b) shows the northern hemisphere. Starting at the center and going outward, latitude decreases from +90° N

to 0° N at the equator. Figure 2-14 (c) shows the southern hemisphere. Starting at the outside of Figure 2-14 (c) and going toward the center, latitude decreases from 0° N to -90° N (+90° S).

Figure 2-15, which was constructed with rgl (Adler 2009) using the R code in Appendix K.17, plots models of Earth horizontal (H) magnetic field intensity for January 1900, 1950, and 2000. The surfaces are 3D polar plots of intensity as radius at angles of longitude and latitude. The plot surface color is direction on the GYRB color wheel. The heavy red, green, and blue lines are, respectively, 0º longitude and latitude, 90º longitude and 0º latitude, and 90º latitude. The bulge near the South Pole appears to be changing shape. Figure 2-16 shows the asymmetry of the Earth main magnetic H field model of 1/1/2000 via 45º rotations about the horizontal red axis, top out of the page.

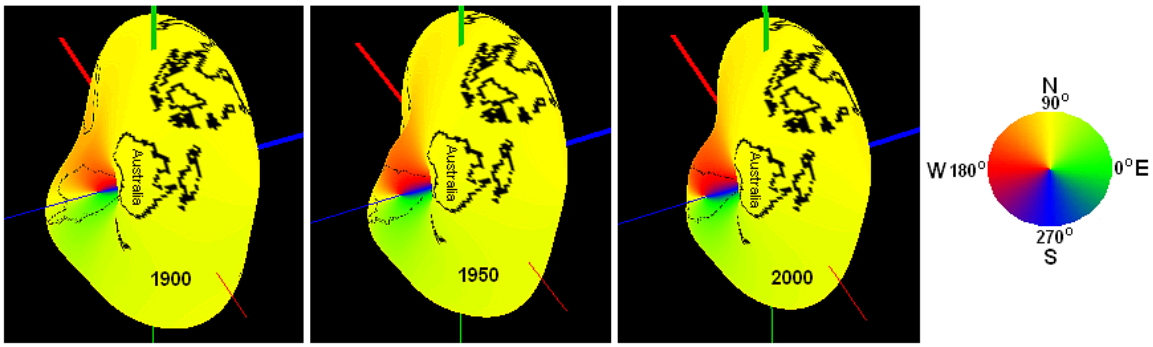

Figure 2-15. 3D Polar Plot of Earth Main Magnetic H Field Model with Direction as a Color and Magnitude as Radius for 1/1/1900, 1/1/1950, and 1/1/2000.

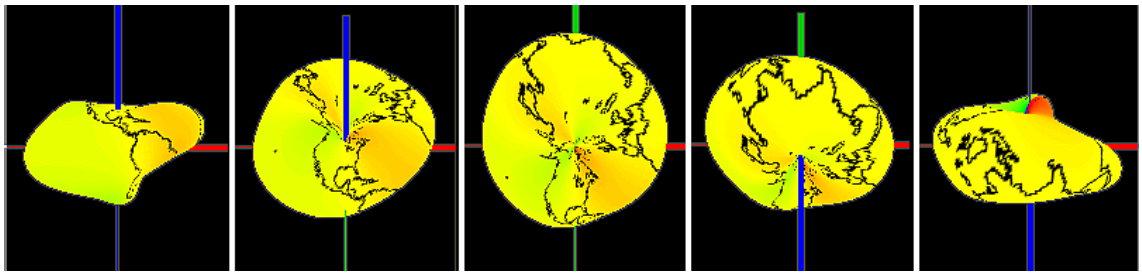

Figure 2-16. Asymmetry of Earth Main Magnetic H Field Model 1/1/2000 Demonstrated by 45º Rotations about the Horizontal Axis Through 0º-180º Longitude at the Equator.

2.8.2 Space Shuttle Solid Rocket Motor Nozzle Internal Flow

Each Space Shuttle is boosted by two solid rocket motors (Figure 2-17a), each 126 feet long and 12 feet in diameter. Figure 2-17 (b) shows an enlarged upper cross section of the nozzle. Gaseous combustion products with entrained liquid aluminum/alumina droplets enter the nozzle at subsonic speeds and accelerate to a Mach number of 1. Maximum compression occurs at the throat where the nozzle internal diameter is minimal. Aft (to the right) of the throat, nozzle diameter increases. Gases exiting the throat to the right expand, increase in velocity to supersonic speeds, and generate thrust.

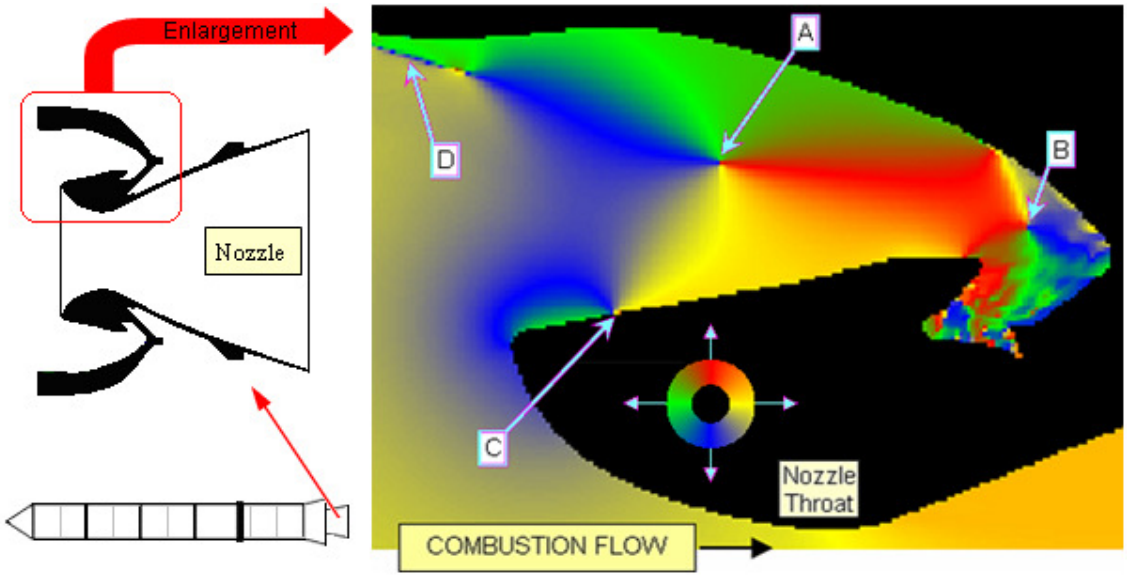

(a) (b)

Figure 2-17. Space Shuttle Booster, Nozzle, and Nozzle Internal Combustion Flow. (a) Space Shuttle solid rocket motor booster and section view of nozzle. (b) enlarged nozzle section (black), YRGB color wheel with direction of flow, and circular dataimage of internal combustion flow. Interesting features include two counter-rotating vortices A and B, flow impingement on the nozzle surface at C, and a narrow particle shear zone at D.

The flow direction imaged in Figure 2-17 (b) was computed with FLUENT, CFD software (FLUENT 2008), for the Space Shuttle solid rocket motor nozzle at 67 seconds from ignition (See Appendix O for permissions). The dataset comprises 30,351 points of four variables (axial and radial coordinates in meters (m), and axial and radial speed in m/sec as computed from the CFD model). With direction of flow aft (right) = yellow, upward = red, forward (left) = green, and down = blue, the large CCW pattern in the cavity above the nozzle throat and centered at point A indicates a CCW flow. The smaller pattern at the right end of the cavity and centered at point B indicates a clockwise flow. These two vortices mesh like oppositely rotating gears. At point C, combustion products flowing down impact the nozzle surface, and rapidly turn forward. D is a high shear zone where particle breakup occurs. The circular dataimage easily shows much more circular-spatial structure than an arrow plot, although an arrow plot is frequently used to plot this rocket nozzle flow data. In particular, an arrow plot easily could miss the narrow high shear zone at D.

2.8.3 Space Shuttle Solid Rocket Motor Nozzle Circular Time Series

Nozzle direction angle is the angle a nozzle is pointing to in the plane perpendicular to the length of the motor (Figure 2-17 (a)). Figure 2-18 (a) shows the red-green-blue-yellow (RGBY) color wheel coding direction. Figure 2-18 (b) images the direction angle of a subset of 176 nozzles from 5 sec to 23 sec after ignition/liftoff in 0.04 second increments. Each narrow horizontal strip is a circular time series of the direction angle of a nozzle. The horizontal strips are vertically ordered to show circular-temporal structure. First, the horizontal strips are ordered vertically by left-side nozzle and right-side nozzle, second by angle in degrees of the Space Shuttle trajectory relative to the Earth equatorial plane, and last by orbital altitude in nautical miles (nm). In bottom half

of Figure 2-18 (b), the dominant red indicates that the left-side nozzle tends to vary about the 0° location, and the dominant blue above indicates that the right-side rocket nozzle tends to vary about the 180° location. This means that the left and right nozzles tend to be pointed toward Earth. The left-side blue vertical band beginning at about 7.5 sec signals the turning of the left-side nozzle to initiate the Space Shuttle roll maneuver as illustrated in Figure 2-19. In Figure 2-18 (a), the red diagonal structure of the right-side nozzle beginning about 15 sec signals the braking of the roll maneuver.

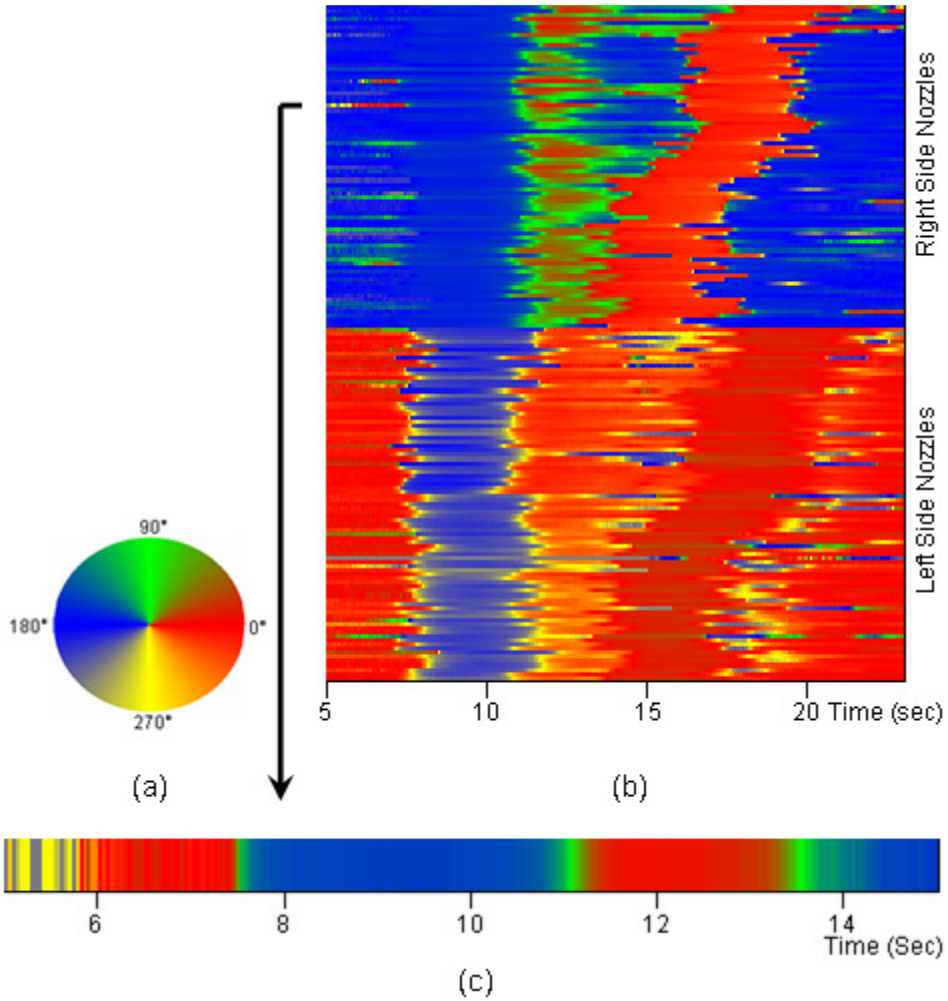

Figure 2-18. Time Series of the Space Shuttle Booster Nozzle Direction Angle. Direction angle is the direction the nozzle is pointing toward in a plane perpendicular to the booster axis. (a) RGBY color wheel, (b) circular time series families, and (c) enlargement of one time series. The vertical and diagonal structures in (b) reflect roll maneuver as influenced by inclination and altitude.

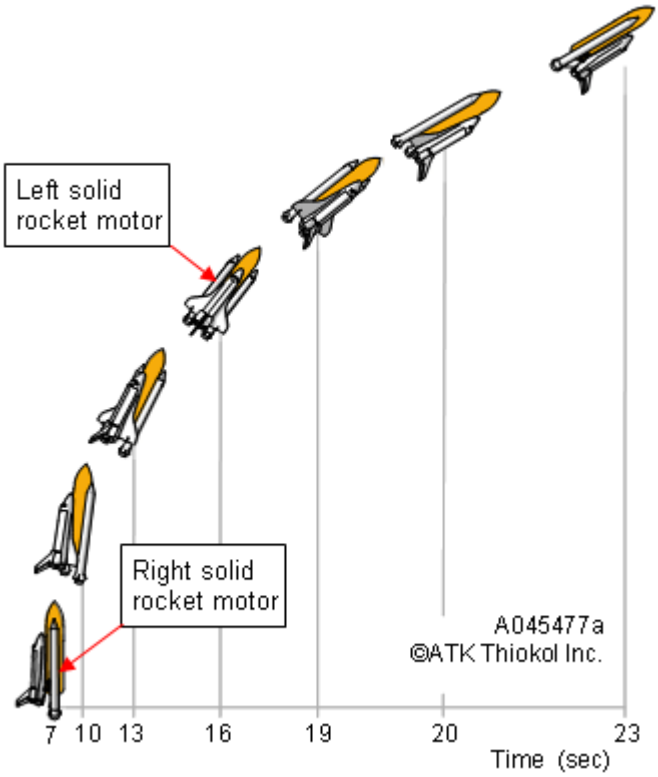

Figure 2-19. Illustration of the Space Shuttle Roll Maneuver vs. Time from Ignition. The time scale is nonlinear to show rotation in equal angular increments.

The diagonal structure in Figure 2-18 (b) from the vertical ordering of the horizontal strips shows a relationship between the nozzle direction angle and inclination and altitude, that without ordering would be obscured by numerical-alpha ordering of the nozzles. Figure 2-18 (c) is an enlargement of the horizontal strip in Figure 2-18 (b) near the tail of the large arrow connecting Figures 2-18 (b) and (c).

The roll maneuver illustrated in Figure 2-19 orients the cargo bay towards the Earth to satisfy communication, scientific, and Space Shuttle engineering requirements, and provides the astronauts with a spectacular view of Earth (Brown 2003).

2.9 Chapter Summary and Future Work

Traditional plots of circular-spatial data become less intelligible as random variation, missing data, and data density increase. These issues were solved by the circular dataimage. The circular dataimage was defined by coding direction as the color at the same angle on a color wheel, with the color wheel defined as a sequence of three or more two-color gradients with the same color between connecting gradients. The circular dataimage eliminated color discontinuity at the cross over point resulting in a continuous image of circular-spatial data, and provided an image in which fine detail on a small scale and large-scale structure on a global scale could be simultaneously recognized. Various suitable color wheels were shown and compared to motivate experimentation, the objective being to effectively contrast and comfortably view interesting circular-spatial structure. The discrete color wheel was constructed from a continuous color wheel by holding color in an angular interval to the start color of a continuous color wheel in the same interval. Variations on circular dataimages were given, e.g., the focus and axial focus plots, with interactive focus on a narrow band of directions or orientations, and direction and magnitude plots including a 3D polar plot with magnitude as radius and direction as color. Examples included global views of average wind direction, internal flow of the Space Shuttle solid rocket motor nozzle, families of circular time series of rocket nozzle vectoring, and the direction of the Earth main magnetic H field.

Future work includes R package CircSpatial implementation of an improved color wheel for deuteranopic color impairment, the focus and axial focus plots (Figures 2-10, 2-11), overlay of magnitude as contour curves (Figure 2-13) and as variable length arrows on circular dataimages, and 3D polar plots (Figure 2-15) with an overlay of features, e.g., geographical boundaries.